

# Green Chemistry

Accepted Manuscript



This is an *Accepted Manuscript*, which has been through the Royal Society of Chemistry peer review process and has been accepted for publication.

*Accepted Manuscripts* are published online shortly after acceptance, before technical editing, formatting and proof reading. Using this free service, authors can make their results available to the community, in citable form, before we publish the edited article. We will replace this *Accepted Manuscript* with the edited and formatted *Advance Article* as soon as it is available.

You can find more information about *Accepted Manuscripts* in the [Information for Authors](#).

Please note that technical editing may introduce minor changes to the text and/or graphics, which may alter content. The journal's standard [Terms & Conditions](#) and the [Ethical guidelines](#) still apply. In no event shall the Royal Society of Chemistry be held responsible for any errors or omissions in this *Accepted Manuscript* or any consequences arising from the use of any information it contains.

**Hydrodeoxygenation of sulfoxides to sulfides by Pt and MoOx co-loaded TiO<sub>2</sub> catalyst**

Abeda Sultana Touchy,<sup>a</sup> S. M. A. Hakim Siddiki,<sup>b</sup> Wataru Onodera,<sup>a</sup> Kenichi Kon,<sup>a</sup> Ken-ichi Shimizu<sup>a,b,\*</sup>

<sup>a</sup> Institute for Catalysis, Hokkaido University, N-21, W-10, Sapporo 001-0021, Japan

<sup>b</sup> Elements Strategy Initiative for Catalysts and Batteries, Kyoto University, Katsura, Kyoto 615-8520, Japan

\*Corresponding author

Ken-ichi Shimizu

Institute for Catalysis, Hokkaido University, N-21, W-10, Sapporo 001-0021, Japan

E-mail: [kshimizu@cat.hokudai.ac.jp](mailto:kshimizu@cat.hokudai.ac.jp), Fax: +81-11-706-9163

**Abstract**

Supported metal nanoparticle catalysts were studied for the hydrodeoxygenation of sulfoxides to sulfides under solvent-free and mild conditions (50-155 °C, 1 or 7 atm H<sub>2</sub>). The catalytic activity for the model reaction of diphenyl sulfoxide depended on the type of metals, support materials and co-loaded oxides of transition metals (V, Nb, Mo, W, Re). Pt and MoOx co-loaded TiO<sub>2</sub> (Pt-MoOx/TiO<sub>2</sub>) showed the highest activity. Pt-MoOx/TiO<sub>2</sub> was reusable after the reaction and was effective for the reduction of various sulfoxides and showed higher turnover number (TON) than previously reported catalysts. Using Pt-MoOx/TiO<sub>2</sub>, benzylphenylsulfone was reduced by H<sub>2</sub> to give phenylbenzyl sulfide via benzylphenyl sulfoxides, which represented the first example of catalytic conversion of a sulfone to a sulfide by H<sub>2</sub>. Characterization studies of Pt-MoOx/TiO<sub>2</sub> show that the surface of TiO<sub>2</sub> is covered by small (or thin layer) Mo oxide species with exposed Mo cations as Lewis acid sites, and 4-5 nm sized Pt metal nanoparticles are supported on the Mo oxides-covered TiO<sub>2</sub>.

**Introduction**

Deoxygenation of sulfoxides to the corresponding sulfides is an important transformation in organic synthesis.<sup>1</sup> Several catalytic methods have been developed to reduce sulfoxides using stoichiometric amount of reducing agents, including silanes,<sup>2</sup> borane,<sup>10,11</sup> phosphine,<sup>12-15</sup> which suffer from use of hazardous reagents and production of by-products that are sometimes difficult to remove from the reaction media. Recently, greener catalytic methods with alcohols<sup>16-20</sup> as reducing agents were developed, but they also suffered from low atom-efficiency. The catalytic deoxygenation of sulfoxides by H<sub>2</sub>, as the most atom-efficient method, is a more challenging reaction, but the previous catalytic methods<sup>21-23</sup> suffer from limited substrate scope, low yields,

low turnover number (TON) and no reports on catalyst reuse. Recently, Mitsudome et al.<sup>24</sup> reported a heterogeneous catalytic system for the deoxygenation of various sulfoxides by 1 atm H<sub>2</sub> using 5 mol% of Ru/TiO<sub>2</sub>, which exhibited a high TON (500) for hydrogeoxygenation of diphenyl sulfoxide. Further improvement in this heterogeneous hydrogeoxygenation method will lead to a greener route to sulfides from sulfoxides. Additionally, hydrogeoxygenation of sulfones to sulfides, which is unprecedented in the literature, is a challenging target in catalysis.

Recently, we found that Pt and MoOx co-loaded TiO<sub>2</sub> (Pt-MoOx/TiO<sub>2</sub>) showed high activity for three types of hydrogenation reactions: (1) catalytic methylation of secondary amines by CO<sub>2</sub> and H<sub>2</sub>,<sup>25</sup> (2) reductive amination of levulinic acid by H<sub>2</sub> to *N*-alkyl-5-methyl-2-pyrrolidones,<sup>26</sup> (3) selective synthesis of primary amines by the reductive amination of ketones.<sup>27</sup> The results motivated us to study a possible application of Pt-MoOx/TiO<sub>2</sub> to the reduction of S=O bonds. Considering that we have not characterized the structure of Pt-MoOx/TiO<sub>2</sub> in detail, estimation of the structure of Pt-MoOx/TiO<sub>2</sub> is an additional issue to be addressed.

We report herein a new catalytic system for the hydrodeoxygenation of various sulfoxides and a sulfone to sulfides under mild conditions (50-155 °C, 1 or 7 atm H<sub>2</sub>) using Pt-MoOx/TiO<sub>2</sub> as a reusable heterogeneous catalyst. Substrate scope, catalyst reuse and catalyst characterization studies are also carried out to show the structure and catalytic performance of Pt-MoOx/TiO<sub>2</sub>.

## Experimental

### General

Commercially available organic and inorganic compounds (from Tokyo Chemical Industry, WAKO Pure Chemical Industries, Kanto Chemical or Mitsuwa Chemical) were used without further purification. GC (Shimadzu GC-2014) and GCMS (Shimadzu GCMS-QP2010) analyses were carried out with Ultra ALLOY capillary column UA<sup>+</sup>-1 (Frontier Laboratories Ltd.) using N<sub>2</sub> and He as the carrier gas.

### Catalyst Preparation

TiO<sub>2</sub> (JRC-TIO-4, 50 m<sup>2</sup> g<sup>-1</sup>), MgO (JRC-MGO-3), CeO<sub>2</sub> (JRC-CEO-3) and HBEA zeolite (JRC-Z-HB25, SiO<sub>2</sub>/Al<sub>2</sub>O<sub>3</sub>= 25±5) were supplied from Catalysis Society of Japan. SiO<sub>2</sub> (Q-10, 300 m<sup>2</sup> g<sup>-1</sup>) was supplied from Fuji Silysia Chemical Ltd. Active carbon (C) was purchased from Kanto Chemical. γ-Al<sub>2</sub>O<sub>3</sub> was prepared by calcination of γ-AlOOH (Catapal B Alumina, Sasol) for 3 h at 900 °C. Nb<sub>2</sub>O<sub>5</sub> was prepared by calcination of Nb<sub>2</sub>O<sub>5</sub>·nH<sub>2</sub>O (supplied by CBMM) at 500 °C for 3 h. ZrO<sub>2</sub> was prepared by hydrolysis of zirconium oxynitrate 2-hydrate by an aqueous NH<sub>4</sub>OH solution, followed by filtration, washing with distilled water, drying at 100 °C for 12 h, and by calcination at 500 °C for 3 h.

Precursors of  $M^1\text{-MoO}_x/\text{TiO}_2$  ( $M^1 = 5 \text{ wt\% Pt, Rh, Pd, Re, Ru, Ni, Cu; 7 wt\% Mo}$ ) and  $\text{Pt-}M^2\text{O}_x/\text{TiO}_2$  ( $5 \text{ wt\% Pt; } M^2 = 7 \text{ wt\% Mo, V, Nb, W, Re}$ ) were prepared by sequential impregnation method using  $M^1$  source [aqueous  $\text{HNO}_3$  solutions of  $\text{Pt}(\text{NH}_3)_2(\text{NO}_3)_2$ ,  $\text{Rh}(\text{NO}_3)_3$  or  $\text{Pd}(\text{NH}_3)_2(\text{NO}_3)_2$ ,  $\text{NH}_4\text{ReO}_4$ ,  $\text{RuCl}_3$  or aqueous solution of nitrates ( $\text{Ni, Cu}$ )],  $M^2$  source [ $(\text{NH}_4)_6\text{Mo}_7\text{O}_{24}\cdot 4\text{H}_2\text{O}$ ,  $\text{NH}_4\text{VO}_3$ , niobium oxalate,  $(\text{NH}_4)_{10}\text{W}_{12}\text{O}_{41}\cdot 5\text{H}_2\text{O}$  or  $\text{NH}_4\text{ReO}_4$ ] and  $\text{TiO}_2$ . For the preparation of  $\text{Pt-MoO}_x/\text{TiO}_2$  ( $5 \text{ wt\% Pt, 7 wt\% Mo}$ ) as an example, 5 g of  $\text{TiO}_2$  and 0.88 mmol of  $(\text{NH}_4)_6\text{Mo}_7\text{O}_{24}\cdot 4\text{H}_2\text{O}$  were added to 50 mL of water at  $50^\circ\text{C}$ , followed by evaporation to dryness at  $50^\circ\text{C}$ , and by drying at  $90^\circ\text{C}$  for 12 h and calcination in air at  $500^\circ\text{C}$  for 3 h to obtain  $\text{MoO}_3$ -loaded  $\text{TiO}_2$  ( $\text{MoO}_3/\text{TiO}_2$ ).  $\text{MoO}_3/\text{TiO}_2$  was added to aqueous  $\text{HNO}_3$  solution of  $\text{Pt}(\text{NH}_3)_2(\text{NO}_3)_2$ , followed by evaporation to dryness at  $50^\circ\text{C}$ , and by drying at  $90^\circ\text{C}$  for 12 h. Precursors of metal oxide-supported Pt catalysts were prepared by the impregnation method using aqueous  $\text{HNO}_3$  solution of  $\text{Pt}(\text{NH}_3)_2(\text{NO}_3)_2$ . Before each catalytic experiment, catalysts were prepared by pre-reduction of the precursor in a pyrex tube under a flow of  $\text{H}_2$  ( $20 \text{ cm}^3 \text{ min}^{-1}$ ) at  $300^\circ\text{C}$  for 0.5 h.

#### Catalyst characterization

X-ray absorption near-edge structures (XANES) at Pt  $L_3$ -edge were measured at the BL14B2 in the SPring-8 (Proposal No. 2012A1734) in a transmittance mode. The storage ring was operated at 8 GeV. A Si(111) double crystal monochromator was used to obtain a monochromatic X-ray beam.  $\text{Pt-MoO}_x/\text{TiO}_2$  pre-reduced in 100%  $\text{H}_2$  ( $20 \text{ cm}^3 \text{ min}^{-1}$ ) for 0.5 h at  $300^\circ\text{C}$  was cooled to room temperature in  $\text{H}_2$  and was sealed in cells made of polyethylene under  $\text{N}_2$ , and then the XANES spectrum was taken at room temperature. XANES analysis was performed using the REX version 2.5 program (RIGAKU).

Oxidation state of Mo species in the pre-reduced  $\text{Pt-MoO}_x/\text{TiO}_2$  was estimated by X-ray photoelectron spectroscopy (XPS) using a JEOL JPS-9010MC ( $\text{MgK}\alpha$  irradiation). Binding energies were calibrated with respect to  $\text{C}_{1s}$  at 285.0 eV.

TEM measurement of the pre-reduced  $\text{Pt-MoO}_x/\text{TiO}_2$  was carried out by using a JEOL JEM-2100F TEM operated at 200 kV.

In situ infrared (IR) spectra were recorded at  $40^\circ\text{C}$  using a JASCO FT/IR-4200 equipped with a quartz IR cell connected to a conventional flow reaction system. The sample was pressed into a 40 mg of self-supporting wafer ( $\phi = 2 \text{ cm}$ ) and mounted into the quartz IR cell with  $\text{CaF}_2$  windows. Spectra were measured accumulating 30 scans at a resolution of  $4 \text{ cm}^{-1}$ . A reference spectrum of the catalyst wafer taken under He at measurement temperature was subtracted from each spectrum. For the IR study of pyridine adsorption on support materials (Fig. 1), the sample disc, pre-heated in He flow at  $500^\circ\text{C}$  for 0.5 h, was exposed to pyridine ( $1 \mu\text{L}$  as liquid) vaporized at  $200^\circ\text{C}$  under He flow at  $200^\circ\text{C}$ . After purging with He for 600 s, IR spectra of adsorbed pyridine were obtained. For the IR study of CO adsorption (Fig. 4), the disk of

Pt-loaded catalysts in situ pre-reduced under  $\text{H}_2$  ( $20 \text{ cm}^3 \text{ min}^{-1}$ ,  $300^\circ\text{C}$ ,  $0.5 \text{ h}$ ), was cooled to  $40^\circ\text{C}$  under He, followed by flowing  $\text{CO}(5\%)/\text{He}$  ( $20 \text{ cm}^3 \text{ min}^{-1}$ ) for  $180 \text{ s}$ . After purging with He ( $40 \text{ cm}^3 \text{ min}^{-1}$ ) for  $600 \text{ s}$ , the IR spectrum of adsorbed CO was obtained.

### Catalytic Tests

$\text{Pt-MoO}_x/\text{TiO}_2$  was used as the standard catalyst. After the pre-reduction at  $300^\circ\text{C}$ , the catalyst in the closed glass tube with a septum inlet was cooled to room temperature under  $\text{H}_2$ . *n*-Dodecane ( $0.05 \text{ g}$ ) was injected to the pre-reduced catalyst inside the glass tube through the septum inlet, then the septum was removed under air, and sulfoxides ( $1.0 \text{ mmol}$ ) and a stirrer bar were charged to the tube, followed by inserting the tube inside a stainless autoclave with a dead space of  $28 \text{ cm}^3$ . Soon after being sealed, the reactor was flushed with  $\text{H}_2$  and charged with  $7 \text{ atm}$   $\text{H}_2$  at room temperature. Then the reactor was heated at  $50$  or  $120^\circ\text{C}$  under stirring ( $180 \text{ rpm}$ ) for  $24 \text{ h}$ . The reactions under ambient  $\text{H}_2$  pressure, eqn. (1) and (2), were carried out in a closed glass tube with balloon hydrogen at  $155^\circ\text{C}$ . For the reactions in Table 1 and Fig. 1, 6, 7, 8 conversions and yields of sulfides were determined by GC using *n*-dodecane as an internal standard adopting the GC-sensitivity estimated using the commercial compounds. For the scope and limitation study in Table 2, isolated yields of products were determined as follows. After the reaction, 2-propanol ( $4 \text{ mL}$ ) was added to the mixture, and the catalyst was separated by centrifugation. Then, the reaction mixture was concentrated under vacuum evaporator to remove the volatile compounds. Then, sulfides were isolated by column chromatography using silica gel 60 (spherical,  $63\text{--}210 \mu\text{m}$ , Kanto Chemical Co. Ltd.) with hexane/ethylacetate ( $2/1$  to  $5/1$ ) as the eluting solvent, followed by analyses by  $^1\text{H}$  NMR,  $^{13}\text{C}$  NMR and GCMS. Concentration of Pt in the solution after the standard reaction was checked by inductive coupling plasma (ICP-AES) using ICPE-9000 (Shimadzu).

## Results and discussion

### Characterization of $\text{Pt-MoO}_x/\text{TiO}_2$

First, we characterized the structure of the  $\text{MoO}_3/\text{TiO}_2$  support. The  $\text{N}_2$  adsorption result showed that the surface area of  $\text{MoO}_3/\text{TiO}_2$  was  $54 \text{ m}^2 \text{ g}^{-1}$ . The XRD pattern of  $\text{MoO}_3/\text{TiO}_2$  showed no diffraction lines due to Mo oxides (result not shown), which indicate the absence of crystalline  $\text{MoO}_3$  particles on  $\text{MoO}_3/\text{TiO}_2$ . According to the literature,<sup>28</sup> the non-crystalline Mo(IV) oxide species on  $\text{TiO}_2$  are monolayer or small clusters (polymeric molybdates) of Mo(IV) oxide. TEM images of  $\text{MoO}_3/\text{TiO}_2$  were also essentially identical to that of  $\text{TiO}_2$ .

Fig. 1 compares IR spectra (the ring-stretching region) of pyridine adsorbed on  $\text{MoO}_3/\text{TiO}_2$  and  $\text{TiO}_2$ . For both of the support materials, strong bands due to the coordinatively bound pyridine on Lewis acid ( $1445$  and *ca*  $1607 \text{ cm}^{-1}$ )<sup>29,30</sup> are observed. The bands for  $\text{MoO}_3/\text{TiO}_2$  are higher in intensity than those for  $\text{TiO}_2$ , which indicates that the relative amount of Lewis acid

sites of  $\text{TiO}_2$  is increased by the loading of  $\text{MoO}_3$ . It is known that the position of the band around  $1607\text{ cm}^{-1}$  increases with increase in the Lewis acid strength of metal oxides.<sup>29</sup> The higher wavenumber of the band for  $\text{MoO}_3/\text{TiO}_2$  ( $1607\text{ cm}^{-1}$ ) than  $\text{TiO}_2$  ( $1604\text{ cm}^{-1}$ ) indicates that Lewis acid strength of  $\text{TiO}_2$  is increased by the loading of  $\text{MoO}_3$ . Considering that the surface density of Mo on  $\text{MoO}_3/\text{TiO}_2$  ( $7.4\text{ Mo atoms nm}^{-2}$ ) is larger than the monolayer coverage of Mo on the  $\text{TiO}_2$  support ( $6\text{ Mo atoms nm}^{-2}$ ),<sup>28</sup> these results suggest that the surface of  $\text{TiO}_2$  is covered by small (or thin layer) polymeric molybdates whose surface contains coordinatively unsaturated Mo cations as Lewis acid sites. This structural model of  $\text{MoO}_3/\text{TiO}_2$  is consistent with that in the literature for  $\text{MoO}_3/\text{TiO}_2$  with a monolayer coverage of Mo.<sup>28</sup> Additionally, the spectrum for  $\text{MoO}_3/\text{TiO}_2$  shows a broad and weak band at  $1538\text{ cm}^{-1}$  due to pyridinium ion ( $\text{PyH}^+$ ) produced by the reaction of pyridine with Brønsted acid site.

Next, the structure of the representative catalyst,  $\text{Pt-MoOx/TiO}_2$  pre-reduced at  $300\text{ }^\circ\text{C}$ , was characterized by various spectroscopic methods. The oxidation state of Mo species was studied by XPS. Fig. 2 compares the XPS spectra (Mo  $3d_{5/2}$  region) of  $\text{MoO}_3/\text{TiO}_2$  and  $\text{Pt-MoOx/TiO}_2$ . As expected, the Mo  $3d_{5/2}$  binding energy (BE) of  $\text{MoO}_3/\text{TiO}_2$  ( $232.6\text{ eV}$ ) corresponds to the oxidation state of  $\text{Mo}^{6+}$ .<sup>31,32</sup> The Mo  $3d_{5/2}$  peak of  $\text{Pt-MoOx/TiO}_2$  appeared at lower BE of  $230.5\text{ eV}$  assignable to  $\text{Mo}^{4+}$  species,<sup>31,32</sup> but peaks due to metallic  $\text{Mo}^0$  ( $227.9\text{ eV}$ )<sup>31</sup> and PtMo alloys ( $227.8\text{ eV}$ )<sup>32</sup> were not observed. Combined with the structural model of  $\text{MoO}_3/\text{TiO}_2$  discussed above, the Mo species on the  $\text{Pt-MoOx/TiO}_2$  catalyst can be small (or thin layer)  $\text{MoO}_2$  species.

The bulk oxidation state of Pt species in  $\text{Pt-MoOx/TiO}_2$  was studied by Pt  $L_3$ -edge XANES (Fig. 3). The XANES feature of  $\text{Pt-MoOx/TiO}_2$  is quite close to that of Pt foil, indicating metallic state of the Pt species in  $\text{Pt-MoOx/TiO}_2$ . The surface oxidation state of Pt species in  $\text{Pt-MoOx/TiO}_2$  was studied by IR spectra of CO adsorbed on the sample (Fig. 4). The IR spectrum of CO adsorbed on  $\text{Pt-MoOx/TiO}_2$  showed a strong band at  $2073\text{ cm}^{-1}$  due to linearly coordinated CO on a metallic  $\text{Pt}^0$  site<sup>32,33</sup> together with a weak band due to bridged CO adspecies on a Pt metal plane ( $1850\text{ cm}^{-1}$ ).<sup>32,33</sup> This indicates that the surface of Pt is metallic.

Fig. 5 shows representative TEM images of  $\text{Pt-MoOx/TiO}_2$ . From low resolution (upper side) and high resolution (lower side) TEM images, the Pt particle size distribution was obtained as shown in the figure. The volume-area mean diameter of Pt particle was  $4.7 \pm 1.1\text{ nm}$ . This value is close to the average diameter of Pt particles ( $4.1\text{ nm}$ )<sup>25</sup> estimated by CO adsorption experiment assuming that CO is adsorbed on the surface of spherical Pt particles at a stoichiometry of  $\text{CO}/(\text{surface Pt atom}) = 1/1$ . Summarizing the structural results, the dominant Pt species in  $\text{Pt-MoOx/TiO}_2$  are around 4-5 nm sized Pt metal nanoparticles. Mo oxides are not observed in the high resolution TEM image, which support that  $\text{MoO}_2$  species on  $\text{Pt-MoOx/TiO}_2$  are small clusters or thin layer species.



### Optimization of catalysts

Table 1 shows the influence of catalyst composition on the catalytic activity for hydrogenation of diphenyl sulfoxide to diphenyl sulfide under solvent-free conditions in 7 atm H<sub>2</sub> at 50 °C for 4 h using 0.1 mol% of the catalyst. Among various Pt catalysts, including bimetal loaded TiO<sub>2</sub> (Pt-MO<sub>X</sub>/TiO<sub>2</sub>; M = 7 wt% Mo, V, Nb, W, Re; entries 2-6), Pt-MoO<sub>x</sub> co-loaded Al<sub>2</sub>O<sub>3</sub> (entry 7) and Pt-loaded metal oxides (entries 8-16), Pt-MoO<sub>X</sub>/TiO<sub>2</sub> (entry 2) showed the highest yield of diphenyl sulfide (97%) as well as the highest conversion of diphenyl sulfoxide (100%). The yield for Pt-MoO<sub>X</sub>/TiO<sub>2</sub> (97%) is much higher than those for MoO<sub>3</sub>/TiO<sub>2</sub> (8%) and Pt/TiO<sub>2</sub> (28%), which indicates synergistic effect between Pt and MoO<sub>3</sub>. Pt-MoO<sub>X</sub>/TiO<sub>2</sub> showed higher yield than the various metal (Rh, Pd, Re, Ru, Ni, Cu)-loaded MoO<sub>X</sub>/TiO<sub>2</sub> catalysts (entries 17-22). Summarizing the screening result, it is found that Pt-MoO<sub>X</sub>/TiO<sub>2</sub> is the best catalyst in the 22 types of the heterogeneous catalysts tested in Table 1. Under the same conditions, Pt-MoO<sub>X</sub>/TiO<sub>2</sub> catalysts with Pt loading of 0.1 and 1 wt% showed 61% and 80% yields (results not shown), which were lower than the standard catalyst with 5 wt% Pt loading.

In our previous studies on the hydrodeoxygenation of carbonyl compounds by Pt-loaded catalysts, we showed that the catalytic activity was highly support-dependent; Lewis acidic supports (such as MoO<sub>X</sub>/TiO<sub>2</sub>) showed higher activity than the other supports.<sup>26,27</sup> The role of the Lewis acid sites is shown to be the activation of C=O bonds by Lewis acid-base interaction between surface Mo cation and carbonyl oxygen, while the Pt is proposed to act as H<sub>2</sub> dissociation site.<sup>26,27</sup> We speculate the same cooperative mechanism of Pt and Lewis acid sites in the present catalytic system, in which Mo cations as Lewis acid sites activate S=O bonds in the substrates.

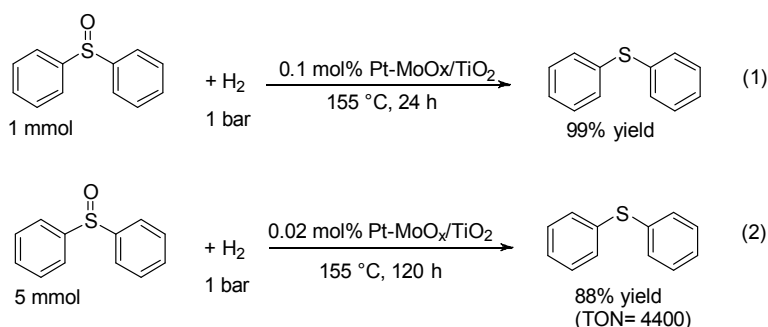
### Catalytic performance of Pt-MoO<sub>X</sub>/TiO<sub>2</sub>

As shown in Fig. 6, the Pt-MoO<sub>X</sub>/TiO<sub>2</sub> catalyst showed good reusability for the hydrogenation of diphenyl sulfoxide under the conditions in Table 1. After the reaction, 2-propanol (4 mL) was added to the mixture, and the catalyst was separated by centrifugation. The catalyst was dried at 100 °C for 1 h and reduced in H<sub>2</sub> at 300 °C for 0.5 h. The recovered catalyst showed high yields (> 89%) of diphenyl sulfide for the next 4 cycles. ICP-AES analysis of the solution after the first reaction showed that the Pt content in the solution was below the detection limits. The results indicate that Pt-MoO<sub>X</sub>/TiO<sub>2</sub> is a reusable heterogeneous catalyst for this reaction.

As summarized in Table 2, the present solvent-free hydrogenation method was applicable to various sulfoxides under 7 atm H<sub>2</sub> at 50 or 120 °C. The reactions of aromatic (entries 1-7), benzylic (entry 8) and aliphatic (entries 9, 10) sulfoxides resulted in the formation of the corresponding sulfides with high isolated yields (85-97%). The method showed chemoselective

hydrogenation of sulfoxides without conversion of other reducible functional groups: Cl- (entry 3), Br- (entry 7), carbonyl (entry 5) groups.

It is important to note that the catalytic system shows high TON under ambient pressure (1 atm) of H<sub>2</sub> in a glass reactor under solvent-free conditions at 155 °C. As shown in eqn. (1), 1 mmol of diphenyl sulfoxide was hydrogenated by Pt-MoO<sub>x</sub>/TiO<sub>2</sub> containing 0.001 mmol (0.01 mol%) of Pt, and diphenyl sulfide was obtained in 99% yield after 24 h. As shown in eqn (2), hydrogenation of 5 mmol of diphenyl sulfoxide in 1 atm H<sub>2</sub> for 120 h by smaller amount of the catalyst (0.02 mol%) gave diphenyl sulfide in 88% yield, corresponding to TON of 4400 with respect to total number of Pt atoms in the catalyst. This value is higher than that of previously reported catalysts.<sup>21-24</sup> However, the reaction of 30 mmol of diphenyl sulfoxide with 0.01 mol% of the catalyst for 120 h resulted in only 28% yield (not shown).



In general, transition metal surfaces interact strongly with sulfur atoms in sulfides, resulting in deactivation of the catalysts. To test sulfur-tolerance of the Pt-MoO<sub>x</sub>/TiO<sub>2</sub> catalyst during the catalytic reaction, we studied the effect of the concentration of a model sulfide, 4-(methylthio)aniline, on the initial formation rate of diphenyl sulfide for hydrogenation of diphenyl sulfoxide by Pt-MoO<sub>x</sub>/TiO<sub>2</sub> (Fig. 7). The reaction rate slightly decreased with the sulfide concentration, but the reaction order with respect to the sulfide ( $n = -0.09$ ) was close to zero. The result indicates that the Pt-MoO<sub>x</sub>/TiO<sub>2</sub> catalyst shows a moderate sulfur-tolerance during the reaction. This sulfur-tolerance may be a possible reason of the high TON of this catalytic system.

Interestingly, the present catalytic system was found to be effective for hydrogenation of a sulfone. Fig. 8 shows a time-yields profile for the reduction of benzyl phenyl sulfone under 7 atm H<sub>2</sub> in the presence of 0.1 mol% of the Pt-MoO<sub>x</sub>/TiO<sub>2</sub> catalyst (containing 0.001 mmol of Pt). The result shows a profile characteristic to consecutive reaction pathway. The yield of un-reacted benzyl phenyl sulfone decreased with time. The yield of the partially hydrogenated product (benzyl phenyl sulfoxides) increased with time and then decreased. After 40 h, a completely deoxygenated product (benzyl phenyl sulfide) was selectively obtained in 85%



yield. To our knowledge, the result represents the first example of catalytic hydrogenation of a sulfone to a sulfide by  $H_2$ .

### Conclusions

Characterization of Pt-MoOx/TiO<sub>2</sub> showed that the surface of TiO<sub>2</sub> was covered by small (or thin layer) MoO<sub>2</sub> species with exposed Mo cations as Lewis acid sites and 4-5 nm sized Pt metal nanoparticles were loaded on the support. Pt-MoOx/TiO<sub>2</sub> was found to be an effective and reusable catalyst for the reduction of sulfoxides to sulfides under solvent-free and mild conditions (50-155 °C, 1 or 7 atm  $H_2$ ), which showed higher TON than previously reported catalysts. Pt-MoOx/TiO<sub>2</sub> catalyzed the reduction of benzyl phenyl sulfone by  $H_2$  to benzyl phenyl sulfide, which represented the first example of catalytic conversion of a sulfone to a sulfide by  $H_2$ .

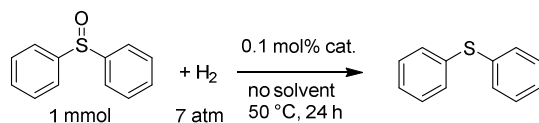
### Acknowledgement

This work was supported by Grant-in-Aids for Scientific Research B (26289299) from MEXT (Japan), a MEXT program “Elements Strategy Initiative to Form Core Research Center” and a Grant-in-Aid for Scientific Research on Innovative Areas “Nano Informatics” (25106010) from JSPS.

## References

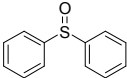
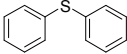
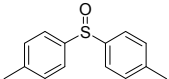
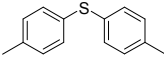
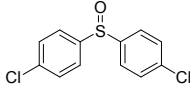
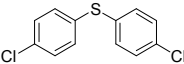
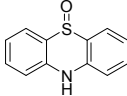
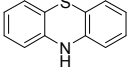
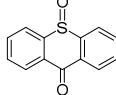
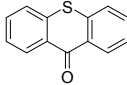
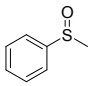
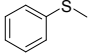
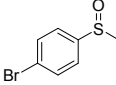
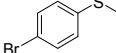
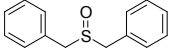
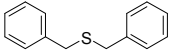
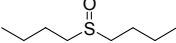
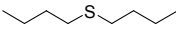
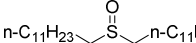
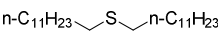
1. a) M. Madesclaire, *Tetrahedron*, 1988, **44**, 6537– 6580; b) R. Hille, *Chem. Rev.*, 1996, **96**, 2757–2816.
2. a) J. H. Enemark, J. J. A. Cooney, J.-J. Wang, R. H. Holm, *Chem. Rev.*, 2004, **104**, 1175–1200; b) J. H. Espenson, *Coord. Chem. Rev.*, 2005, **249**, 329–341.
3. A. C. Fernandes and C. C. Romão, *Tetrahedron*, 2006, **62**, 9650–9654.
4. I. Cabrita, S. C. A. Sousa and A. C. Fernandes, *Tetrahedron Lett.*, 2010, **51**, 6132–6135.
5. S. Enthaler, *Catal. Sci. Technol.*, 2011, **1**, 104–110.
6. S. Enthaler, *ChemCatChem*, 2011, **3**, 666–670.
7. S. Krackl, A. Company, S. Enthaler and M. Driess, *ChemCatChem*, 2011, **3**, 1186–1192.
8. Y. Mikami, A. Noujima, T. Mitsudome, T. Mizugaki, K. Jitsukawa and K. Kaneda, *Chem. Eur. J.*, 2011, **17**, 1768–1722.
9. J. M. S. Cardoso and B. Royo, *Chem. Commun.*, 2012, **48**, 4944–4946.
10. A. C. Fernandes and C. C. Romão, *Tetrahedron Lett.*, 2007, **48**, 9176–9179.
11. S. Enthaler, S. Krackl, E. Irran and S. Inoue, *Catal. Lett.*, 2012, **142**, 1003–1010.
12. Z. Zhu and J. H. Espenson, *J. Mol. Catal. A*, 1995, **103**, 87–94.
13. J. B. Arterburn and M. C. Perry, *Tetrahedron Lett.*, 1996, **37**, 7941–7944.
14. R. Sanz, J. Escribano, R. Aguado, M. R. Pedrosa and F. J. Arnáiz, *Synthesis*, **2004**, 1629–1632.
15. M. Bagherzadeh, M. M. Haghdooost, M. Amini and P. G. Derakhshandeh, *Catal. Commun.*, 2012, **23**, 14–19.
16. N. García, P. García-García, M. A. Fernández-Rodríguez, R. Rubio, M. R. Pedrosa, F. J. Arnáiz and R. Sanz, *Adv. Synth. Catal.*, 2012, **354**, 321–327.
17. S. C. A. Sousa, J. R. Bernardo and A. C. Fernandes, *Tetrahedron Lett.*, 2012, **53**, 6205–6208.

18. S. C. A. Sousa, J. R. Bernardo, P. R. Florindo and A. C. Fernandes, *Catal. Commun.*, 2013, **40**, 134–138.
19. N. García, P. García- García, M. A. Fernández-Rodríguez, D. García, M. R. Pedrosa, F. J. Arnáiz and R. Sanz, *Green Chem.*, 2013, **15**, 999–1005.
20. Y. Takahashi, T. Mitsudome, T. Mizugaki, K. Jitsukawa and K. Kaneda, *Chem. Lett.*, 2014, **43**, 420–422.
21. K. Ogura, M. Yamashita and G. Tsuchihashi, *Synthesis*, **1975**, 385–387.
22. B. R. James, F. T. T. Ng and G. L. Rempel, *Can. J. Chem.*, 1969, **47**, 4521–4526.
23. P. M. Reis, P. J. Costa, C. C. Romão, J. A. Fernandes, M. J. Calhorda and B. Royo, *Dalton Trans.*, **2008**, 1727–1733.
24. T. Mitsudome, Y. Takahashi, T. Mizugaki, K. Jitsukawa and K. Kaneda, *Angew. Chem. Int. Ed.*, 2014, **53**, 8348–8351.
25. K. Kon, S. M. A. H. Siddiki, W. Onodera and K. Shimizu, *Chem. Eur. J.*, 2014, **20**, 6264–6267.
26. A. S. Touchy, S. M. A. H. Siddiki, K. Kon and K. Shimizu, *ACS Catal.*, 2014, **4**, 3045–3050.
27. Y. Nakamura, K. Kon, A. S. Touchy and K. Shimizu, *ChemCatChem*, 2015, **7**, 921–924.
28. G. Tsilomelekis and S. Boghosian, *J. Phys. Chem. C*, 2011, **115**, 2146–2154.
29. D. T. Lundie, A. R. McInroy, R. Marshall, J. M. Winfield, P. Jones, C. C. Dudman, S. F. Parker, C. Mitchell and D. Lennon, *J. Phys. Chem. B*, 2005, **109**, 11592–11601.
30. M. Tamura, K. Shimizu and A. Satsuma, *Appl. Catal. A*, 2012, **433–434**, 135–145.
31. A. Katrib, J. W. Sobczak, M. Krawczyk, L. Zommer, A. Benadda, A. Jablonski and G. Maire, *Surf. Interface Anal.*, 2002, **34**, 225–229.
32. S. Zafeiratos, G. Papakonstantinou, M. M. Jacksic and S. G. Neophytides, *J. Catal.*, 2005, **232**, 127–136.
33. D. A. G. Aranda and M. Schmal, *J. Catal.*, 1997, **171**, 398–405.

**Table 1.** Catalyst screening for hydrogenation of diphenyl sulfoxide to diphenyl sulfide.

Entry	Catalysts	Conv. (%)	GC yield (%)
1	MoO <sub>3</sub> /TiO <sub>2</sub>	9	8
2	Pt-MoO <sub>x</sub> /TiO <sub>2</sub>	100	97
3	Pt-ReO <sub>x</sub> /TiO <sub>2</sub>	69	67
4	Pt-WO <sub>x</sub> /TiO <sub>2</sub>	56	54
5	Pt-NbO <sub>x</sub> /TiO <sub>2</sub>	41	40
6	Pt-VO <sub>x</sub> /TiO <sub>2</sub>	37	36
7	Pt-MoO <sub>x</sub> /Al <sub>2</sub> O <sub>3</sub>	73	71
8	Pt/Al <sub>2</sub> O <sub>3</sub>	58	56
9	Pt/Nb <sub>2</sub> O <sub>5</sub>	56	54
10	Pt/HBEA	48	47
11	Pt/MgO	42	39
12	Pt/CeO <sub>2</sub>	41	38
13	Pt/ZrO <sub>2</sub>	34	31
14	Pt/TiO <sub>2</sub>	30	28
15	Pt/SiO <sub>2</sub>	25	23
16	Pt/C	25	24
17	Rh-MoO <sub>3</sub> /TiO <sub>2</sub>	75	72
18	Pd-MoO <sub>3</sub> /TiO <sub>2</sub>	57	55
19	Re-MoO <sub>3</sub> /TiO <sub>2</sub>	40	39
20	Ru-MoO <sub>3</sub> /TiO <sub>2</sub>	34	33
21	Ni-MoO <sub>3</sub> /TiO <sub>2</sub>	26	24
22	Cu-MoO <sub>3</sub> /TiO <sub>2</sub>	15	14

**Table 2.** Pt-MoO<sub>x</sub>/TiO<sub>2</sub>-catalyzed sulfides synthesis from various sulfoxides.

$  \begin{array}{c}  \text{O} \\  \parallel \\  \text{R}^1\text{S}-\text{R}^2 \\  1 \text{ mmol}  \end{array}  + \text{H}_2  \xrightarrow[\text{no solvent, } 120^\circ\text{C, 24 h}]{0.1 \text{ mol\% Pt-MoO}_x/\text{TiO}_2, 7 \text{ atm}}  \begin{array}{c}  \text{R}^1\text{S}-\text{R}^2  \end{array}  $			
Entry	Sulfoxide	Sulfide	Isolated yield (%)
1 <sup>a</sup>			97
2			92
3			88
4			87
5			85
6			94
7			91
8 <sup>b</sup>			96
9			98 <sup>c</sup>
10			91

<sup>a</sup> T = 50 °C, <sup>b</sup> t = 36 h, <sup>c</sup> GC yield

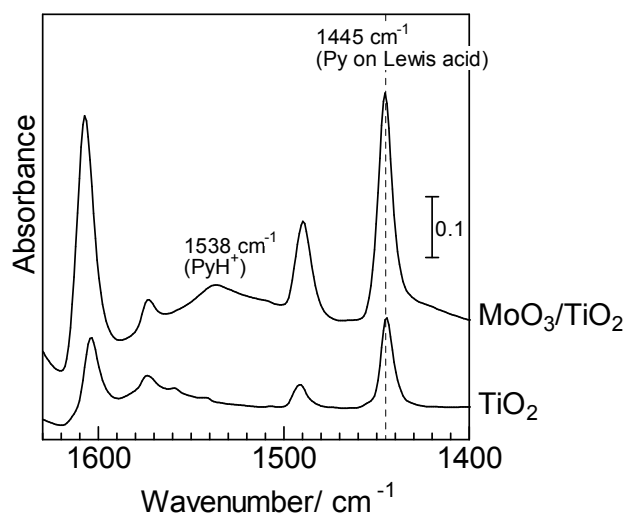


**Fig. 1** IR spectra of pyridine adsorbed on support materials (40 mg) at 200 °C

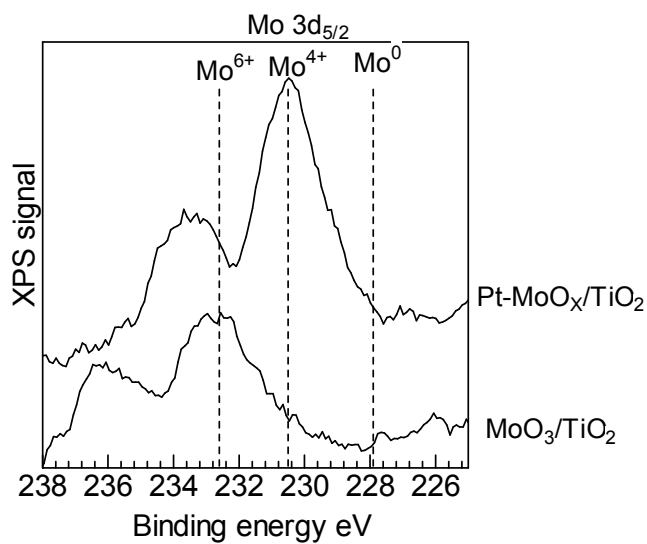


**Fig. 2** XPS spectra of Mo 3d region of  $\text{MoO}_3/\text{TiO}_2$  and  $\text{Pt-MoO}_x/\text{TiO}_2$ .

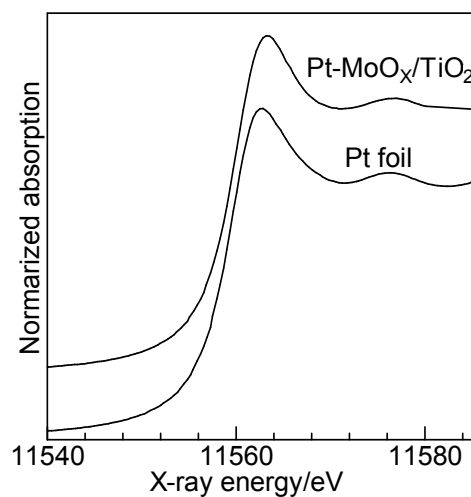


**Fig. 3.** Pt L<sub>3</sub>-edge XANES spectra of Pt-MoO<sub>x</sub>/TiO<sub>2</sub> and Pt foil.

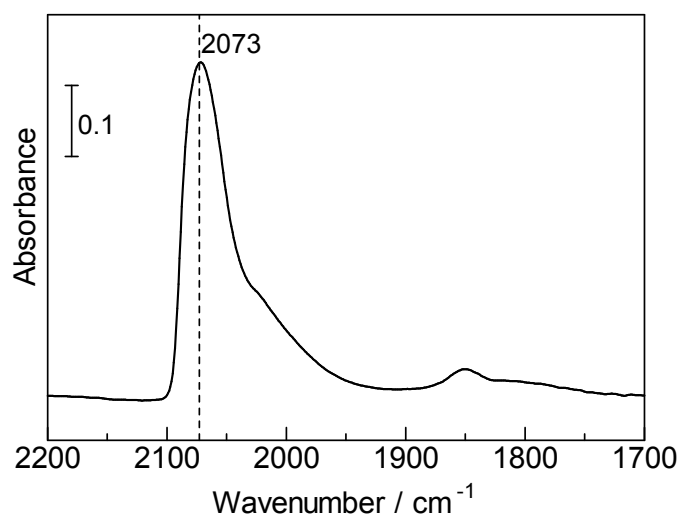


**Fig. 4.** IR spectra of CO adsorbed on Pt-MoO<sub>x</sub>/TiO<sub>2</sub> at 40 °C.



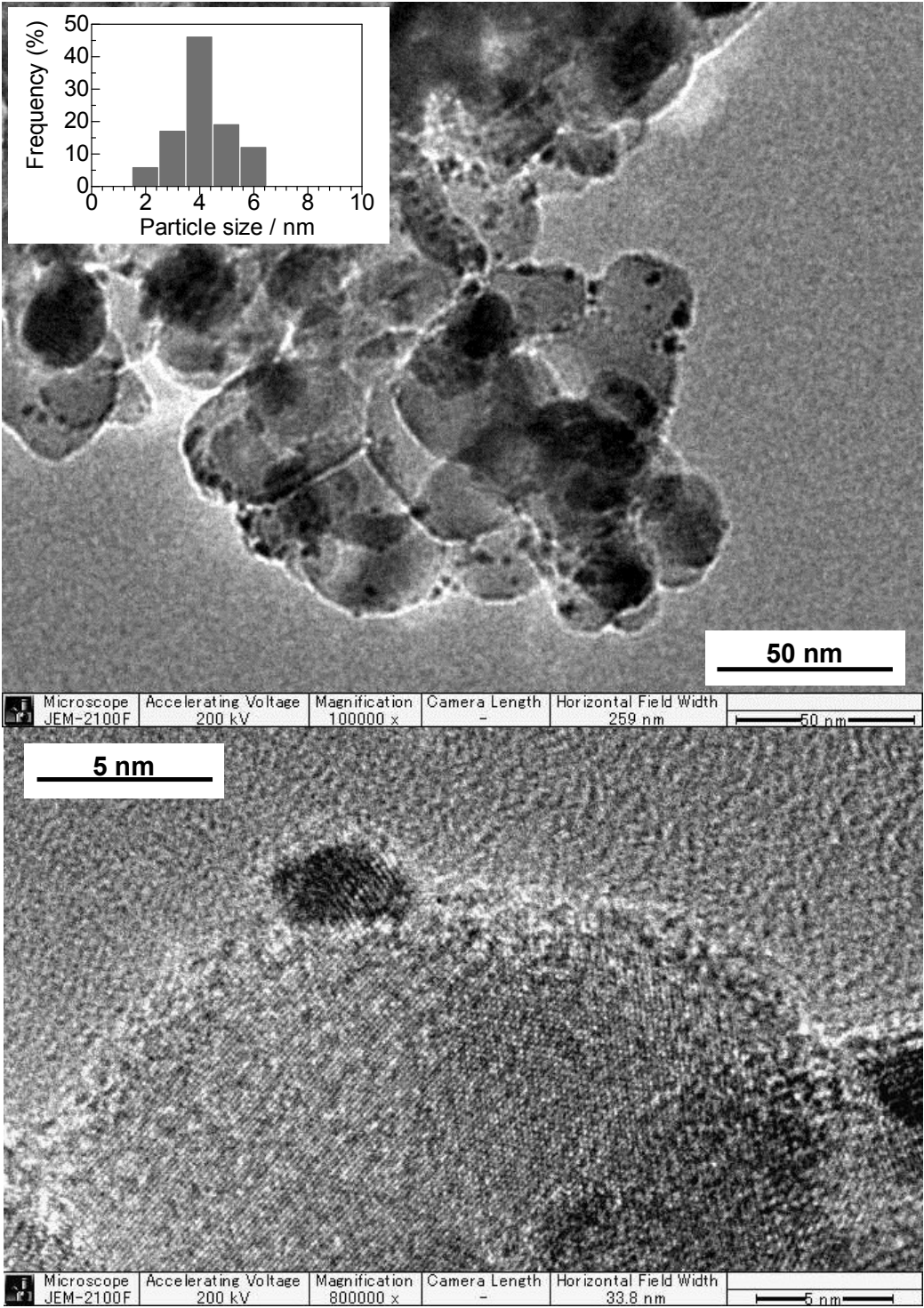


**Fig. 5** Representative TEM images and Pt particle size distribution of Pt-MoO<sub>x</sub>/TiO<sub>2</sub>. The volume-area mean diameter of Pt particle was 4.7 ± 1.1 nm.

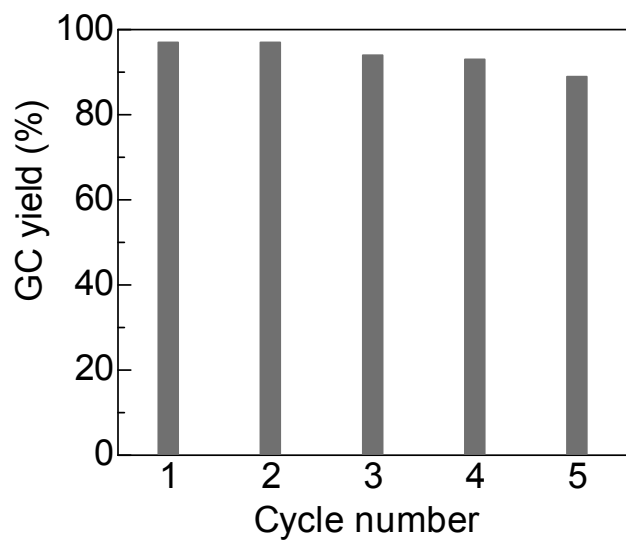


**Fig. 6** Catalyst reuse for hydrogenation of diphenyl sulfoxide to diphenyl sulfide.

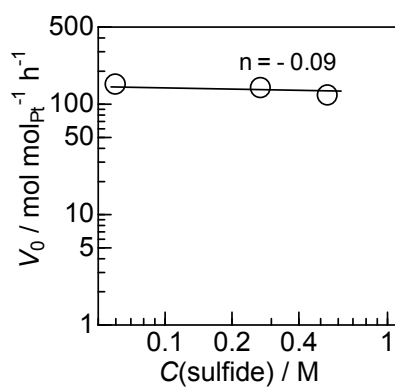


**Fig. 7** Initial formation rate of diphenyl sulfide vs concentration of a sulfide, 4-(methylthio)aniline, for hydrogenation of diphenyl sulfoxide to diphenyl sulfide at 50 °C under 7 atm  $\text{H}_2$  by 0.1 mol% Pt-MoOx/TiO<sub>2</sub>.

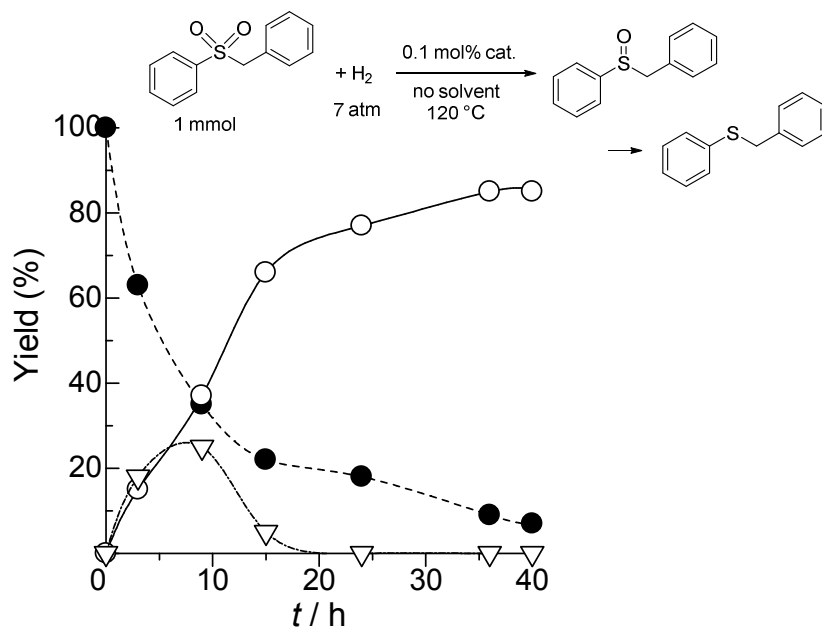


**Fig. 8** Time dependence of GC yields for the reduction of benzyl phenyl sulfone at 120 °C under 7 atm H<sub>2</sub> by 0.1 mol% Pt-MoO<sub>x</sub>/TiO<sub>2</sub> catalyst: (●) unreacted benzyl phenyl sulfone, (▽) benzyl phenyl sulfoxide, (○) benzyl phenyl sulfide.

## Table of Contents

We report the first reusable catalyst for hydrodeoxygenation of various sulfoxides to sulfide as well as the first example of hydrodeoxygenation of a sulfone to a sulfide.

